Journal of Solid State Chemistry 181 (2008) 2859–2863

Contents lists available at ScienceDirect

Journal of Solid State Chemistry

journal homepage: www.elsevier.com/locate/jssc

The layered metal Ti_2PTe_2

Frauke Philipp [a], Peer Schmidt [a,*], Michael Ruck [a], Walter Schnelle [b], Anna Isaeva [c]

[a] Department of Chemistry and Food Chemistry, Dresden University of Technology, Helmholtzstr. 10, 01069 Dresden, Germany
[b] Max-Planck Institute for Chemical Physics of Solids, Nöthnitzer Street 40, 01187 Dresden, Germany
[c] Material Science Department, Moscow State University, 119991 Leninskie Gory, 1, Moscow, Russia

ARTICLE INFO

Article history:
Received 8 May 2008
Received in revised form
7 July 2008
Accepted 16 July 2008
Available online 22 July 2008

In memoriam of Boris Aleksandrovich Popovkin

Keywords:
Titanium phosphide telluride
Crystal structure
XANES-fluorescence
Electrical conductivity
Band structure

ABSTRACT

Crystals of Ti_2PTe_2 have been synthesised by chemical vapour transport. Ti_2PTe_2 crystallises, isostructural to the mineral tetradymite (Bi_2STe_2), in the space group $R\bar{3}m$ with unit-cell parameters $a = 3.6387(2)$ Å and $c = 28.486(2)$ Å for the hexagonal setting. In the structure, layers of isolated phosphide and telluride anions form an ordered close sphere-packing with titanium cations filling two-thirds of the octahedral voids. From XANES fluorescence, the presence of Ti^{4+} is clearly established. In accordance with the ionic formula $(Ti^{4+})_2(P^{3-})(Te^{2-})_2(e^-)$ metallic conductivity ($\rho = 40\,\mu\Omega$ cm at 300 K) and nearly temperature-independent paramagnetism are found. The electronic band structure shows bands of titanium states crossing the Fermi level in directions corresponding to the *ab*-plane and a band gap along the *c*-axis.

1. Introduction

Although many ternary metal pnictide chalcogenides such as antimonide selenides [1–5], antimonide tellurides [4–19], arsenide selenides [4,18–31], arsenide tellurides [18,30–37] and even phosphide sulphides [6,18,29,38–42] and phosphide selenides [4,18,23,40–42] exist, by now only a small number of phosphide tellurides are known. Among these, only the compound UPTe contains separated phosphide and telluride anions. It crystallises in the $LaSb_2$ structure type, which is closely related to the PbFCl structure type [43,44]. In this structure, square-net layers of phosphide or telluride anions are separated by the uranium cations. Compounds like IrPTe (paracostibite type) [45], OsPTe (arsenopyrite type) and RuPTe (crystal structure unknown) [46] contain $[P–Te]^{3-}$-dumbbells, which has been proved by infra-red spectroscopy, and thus they have to be called telluridophosphides. Another representative for ternary compounds with the anionic part consisting of phosphorus and tellurium is BaP_4Te_2, which is built up from barium cations and $^1_\infty[P_4Te_2]^{2-}$-anions [47].

We succeeded in synthesising Ti_2PTe_2, the second metal phosphide telluride containing only single-atomic anions. The thermodynamic properties of the compound have been reported elsewhere [48]; here, the crystal structure, the physical properties and results of quantum chemical calculations will be presented.

2. Experimental section

Ti_2PTe_2 has been synthesised by heating a stoichiometric mixture of tellurium (Acros, 99.8%), red amorphous phosphorus (Fluka, 99%, washed according to [49]) and titanium (Alfa Aesar, 99.9%) in a sealed, evacuated silica tube up to 1123 K at a heating rate of 10 K h^{-1}, keeping this temperature for 1 day, and cooling the mixture down to 673 K at a cooling rate of 1 K h^{-1}. An alternative way of synthesis is the reduction of either P_2O_5 (Laborchemie Apolda, 99%, sublimed) and TeO_2 (Alfa Aesar, ultrapure), or $Te_8O_{10}(PO_4)_4$ (synthesised according to [50]) with elemental titanium to Ti_2O_3 and the desired compound. It was separated from the resulting mixture Ti_2O_3+Ti_2PTe_2 by chemical vapour transport. The transport reaction was performed in a temperature gradient from 973 to 873 K applied by a two-zone furnace over a transport length of approximately 12 cm by adding traces of $TeCl_{4(s)}$ to the reaction mixture [compare 48]. The crystals exhibit a dark grey colour with metallic lustre and form hexagonal-shaped platelets, which are stable in air for at least 1 year. As in EDX-measurements only the elements Ti, Te and P and no Si have been detected, and as the tubes never were attacked by the reaction mixture it is assumed that no silicon has been incorporated in the compound.

* Corresponding author. Fax: +49 351 463 37287.
E-mail address: peer.schmidt@chemie.tu-dresden.de (P. Schmidt).
URL: http://www.peer-schmidt.de (P. Schmidt).

0022-4596/$ - see front matter © 2008 Elsevier Inc. All rights reserved.
doi:10.1016/j.jssc.2008.07.018

Table 1
Crystallographic data and details of the structure determination for Ti_2PTe_2 at 293(1) K and unit-cell parameters for the hexagonal cell determined from X-ray powder diffraction data

Formula	Ti_2PTe_2
Crystal system, space group	Rhombohedral, $R\bar{3}m$ (no. 166)
Unit-cell parameters	$a = 3.6387(2)$ Å, $c = 28.486(2)$ Å, $V = 326.63(3)$ Å^3
Formula units per cell	$Z_{hexagonal} = 3$
Calculated density	$\rho = 5.825\,g\,cm^{-3}$
Crystal size	0.2 mm × 0.2 mm × 0.1 mm
Measurement device	Imaging plate diffractometer IPDS-I (Stoe)
Radiation	Graphite-monochromated Mo$K\alpha$ ($\lambda = 0.71073$ Å)
Measurement limits	$2\theta \leqslant 54.91^\circ$; $-4 \leqslant h$, $k \leqslant 4$; $-5 \leqslant l \leqslant 36$
Absorption correction	Numerical; crystal description optimised using sets of equivalent reflections
Absorption coefficient	μ (Mo$K\alpha$) = 16.8 mm^{-1}
Transmission factors	0.095–0.150
Number of reflections	1037 measured, 130 independent
Data averaging	$R_{int} = 0.046$, $R_\sigma = 0.031$
Structure refinement	Full-matrix least-squares on F_o^2, anisotropic displacement parameters
Extinction parameter	0.021(2)
Refined parameters	10
Residual electron density	2.11 to −1.64 e$^-$ Å^{-3}
Figures of merit	R_1(all F_o) = 0.025; wR_2 (all F_o^2) = 0.055

Table 2
Wyckoff positions, coordinates and coefficients U_{ij} (Å^{-2}) of the anisotropic displacement parameters according to $\exp\{-2\pi^2[U_{11}h^2a^{*2}+\cdots+2U_{23}klb^*c^*]\}$ for Ti_2PTe_2

Atom	W.p.	x	y	z	$U_{11} = U_{22}$	U_{33}	U_{eq}
P	3*a*	0	0	0	0.004(1)	0.007(2)	0.0051(8)
Ti	6*c*	0	0	0.37975(6)	0.0071(7)	0.0065(9)	0.0069(5)
Te	6*c*	0	0	0.77669(2)	0.0080(5)	0.0069(5)	0.0076(5)

$U_{13} = U_{23} = 0$; $U_{12} = U_{11}/2$.

Suitable single crystals for X-ray investigations have been selected by taking precession photographs. Single-crystal data were collected on an imaging plate diffractometer (Stoe IPDS-I). The microscopic crystal description was optimised using sets of symmetry equivalent reflections [51] and then used in a numerical absorption correction [52].

The crystal structure was solved in the space group $R\bar{3}m$ (no. 166) by direct methods and refined against values of F_o^2 (SHELXL-97 [53]). The unit-cell parameters $a = 3.6387(2)$ Å and $c = 28.486(2)$ Å for the hexagonal setting have been determined based on X-ray powder diffraction data (Cu$K\alpha_1$, Stoe Stadi P diffractometer). Details of the data collection and the structure solution are gathered in Tables 1 and 2.

XANES measurements in fluorescence mode have been performed at the beam-line E4 at HASYLAB, DESY, Hamburg. A germanium detector cooled with liquid nitrogen was used. The absorption spectra have been recorded on the energy range from 4.9 to 5.5 keV.

Electrical resistivity was measured between 4 and 320 K on an elongated hexagonal crystal platelet (approximately $1.0 \times 0.5 \times 0.03$ mm^3) by a four-point dc method. The current contacts covered the small faces while the voltage contacts were on top of the crystal. With this arrangement the in-plane resistivity was determined. The estimated inaccuracy in $\rho(T)$ of $\pm 50\%$ is due to the determination of the contact geometry. The determination of $\rho(T)$ perpendicular to the platelet failed due to internal short-circuits between the planes of the crystal.

Magnetisation was measured in fields between 100 and 70 kOe, and for temperatures between 1.8 and 400 K in a SQUID magnetometer (MPMS-XL7, Quantum Design). A microcrystalline sample with $m \approx 67$ mg was contained in a calibrated quartz tube. It was not possible to measure magnetisation on ground single crystals as the vapour transport rate is too low to get sufficient amount of crystals [compare 48].

The DFT electronic structure calculations for Ti_2PTe_2 were performed with the CRYSTAL98 [54] programme package employing the hybrid B3LYP exchange correlation potential. The Hay–Wadt effective large-core pseudo-potentials (HAYWLC) and valence basis sets [55] were used unchanged for phosphorous and tellurium. The Hay–Wadt small-core effective core potential (HAYWSC) and valence basis set utilised in [56] were introduced for titanium. The effective core potentials (ECPs) and basis sets for titanium and phosphorus were previously tested in the calculations of titanium metal and several titanium phosphides and proved to represent the main features of their electronic structures correctly. The reliability of the Hay–Wadt basis set and ECP for tellurium is already confirmed in similar calculations [57]. The convergence criterion for the self-consistent field energy was set to 10^{-7} hartree. For the visualisation of the density of states (DOS) curves and the band structure the XCrysDen programme [58] was used.

3. Results and discussion

3.1. Crystal structure

Ti_2PTe_2 has the Bi_2STe_2 structure type [59]. Here, the hexagonal setting of the space group $R\bar{3}m$ is used as it enables a better recognition of the structural motives; the representation of the rhombohedral cell with angles much lower than 90° is confusing. In the structure, the phosphide as well as the telluride anions are arranged in hexagonal layers, which are stacked along the hexagonal *c*-axis in a sequence with two layers of telluride ions followed by one layer of phosphide ions (Fig. 1). The octahedral voids between phosphide and telluride ions are filled by titanium cations. Since the voids between neighbouring telluride layers remain empty, sandwich layers [Te–Ti–P–Ti–Te] result, which are separated by van der Waals gaps. The individual sandwich layer can be interpreted as a section from a superstructure of the NaCl type. In other words, the anions form an ordered close sphere-packing with the same stacking order (ABABCBCAC) as known from elemental samarium [62]. The titanium cations fill two-thirds of the octahedral voids of this packing. These titanium positions as well as the phosphorus and tellurium positions were found to be fully occupied.

The same structural principle has been reported for some mixed chalcogenides, like Bi_2SeTe_2 [60] and Sb_2SeTe_2 [61]. Furthermore, there are compounds with the same stacking sequence, but partially or completely filled octahedral voids between the sandwich layers, for example $Zr_{0.29}Zr_2AsTe_2$ or $NaZr_2AsTe_2$ [34].

In the crystal structure of Ti_2PTe_2, the interatomic distance Ti–P is 2.4823(9) Å. The Ti$^-$Te distance in Ti_2PTe_2 (2.774(2) Å) is very similar as in the likewise layered binary compound $TiTe_2$ (2.715 Å [63]). Tellurium atoms that follow each other in adjacent layers are separated by 3.859(1) Å. This distance is longer than in the structural-related compound Bi_2SeTe_2 (3.6655 Å; [60]), where the larger bismuth cations expand the layers in the hexagonal plane. Thus, the distance between tellurium atoms in one layer increases, so that the tellurium atoms in adjacent layer can come closer.

3.2. XANES measurements at the titanium K-edge

XANES measurements were used to get clarification of the oxidation state of titanium in Ti_2PTe_2. It was not possible to measure the spectra in standard absorption mode due to the overlap of the Ti–*K*-edge at 4966 eV and the Te–L_1-edge at 4939 eV. Therefore, fluorescence measurements perpendicular to the primary beam were applied. The position of the absorption edge is dependent on the oxidation state of the pertinent element, where species with high oxidation states shift the edge to higher energies. Determination of oxidation states is possible by comparison with spectra of compounds of known oxidation states.

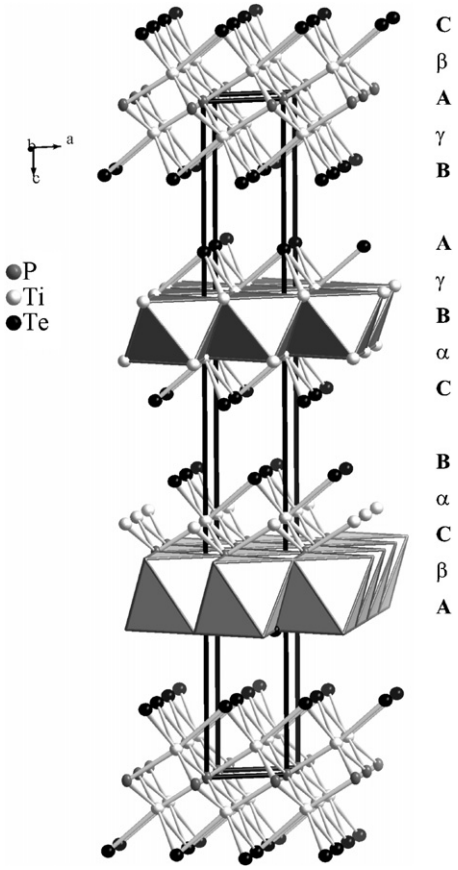

Fig. 1. Crystal structure of Ti_2PTe_2 with stacking sequence of the hexagonal layers of anions (Latin capital letters) and cations (Greek letters). Highlighted in dark is the octahedral coordination of phosphorus by titanium, and in light the octahedral coordination of titanium by phosphorus and tellurium.

The absorption edges of titanium in Ti_2PTe_2 and in TiO_2 (rutile) appear at similar energies while the one of titanium in Ti_2O_3 is shifted to lower energy. The small shift of the absorption edge of Ti_2PTe_2 related to the one of TiO_2 could be related to a small difference in electronegativity between titanium and as well phosphorus as tellurium compared with the difference in electronegativity between titanium and oxygen.

If the absorption edge of titanium in Ti_2PTe_2 is compared with the ones of titanium in the binaries tellurides $Ti^{4+}Te_2$ and $Ti^{3+}{}_2Te_3$ and the binary phosphide $Ti^{3+}P$, it is found in the same energy region as the one of $TiTe_2$, while the edges of Ti_2Te_3 and TiP are shifted clearly to lower energies (Fig. 2). This indicates that the oxidation state of titanium is similar in Ti_2PTe_2 and in $TiTe_2$. The latter compound was found to be metallic due to an overlap of Te–*p*-block bands with Ti–*d*-block bands, and therefore has to be described as $Ti^{(4-\varepsilon)+}(Te^{(2-\varepsilon/2)-})_2$ instead of $Ti^{4+}(Te^{2-})_2$ [64]. Anyway, the oxidation state must be much closer to Ti^{4+} than to Ti^{3+}. In summary the XANES measurements show that the oxidation state of titanium in Ti_2PTe_2 is well described as (4+).

3.3. Physical properties

The magnetic susceptibility of Ti_2PTe_2 is weakly paramagnetic (Fig. 3). At low temperatures, a minor Curie-paramagnetic contribution due to paramagnetic impurities and/or crystal defects is visible. Extrapolating the weak temperature dependence of $\chi(T)$ to $T = 0$ K a value $\chi_0 = +20 \times 10^{-6}$ emu mol^{-1} is found. With the sum of the diamagnetic contributions ($\approx -150 \times 10^{-6}$ emu mol^{-1} [65]), a Pauli-paramagnetic term $\chi_P \approx +170 \times 10^{-6}$ emu mol^{-1} is derived. This corresponds to an electronic DOS at the Fermi-level DOS(E_F) of ≈ 5.3 states eV^{-1}. No phase transitions or superconductivity was detected above 1.8 K and in fields as low as 100 Oe.

The in-plane electrical resistivity displays clearly metal-like temperature dependence (Fig. 4). The value at room temperature ($\rho \approx 40\,\mu\Omega$ cm) is remarkably of the same order as for titanium

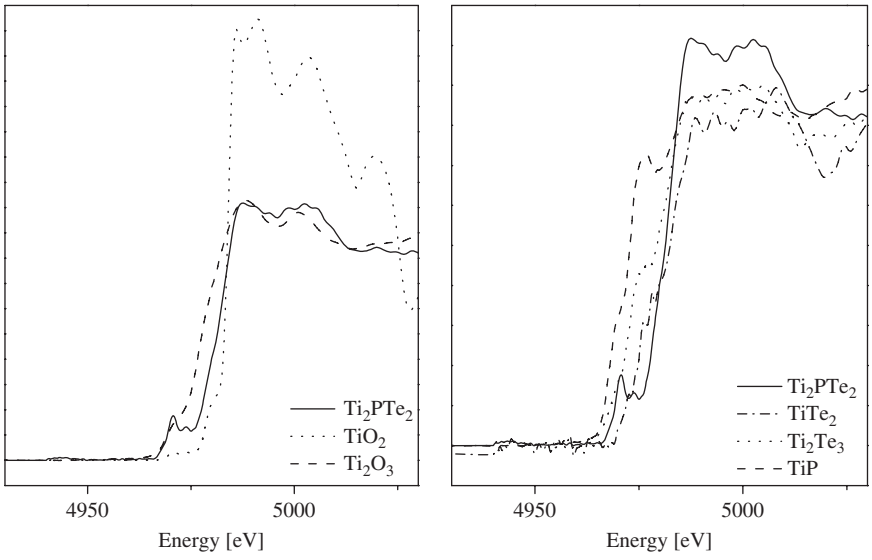

Fig. 2. X-ray absorption spectrum of Ti_2PTe_2 in comparison to Ti_2O_3 and TiO_2 (left) and to $TiTe_2$, Ti_2Te_3 and TiP (right).

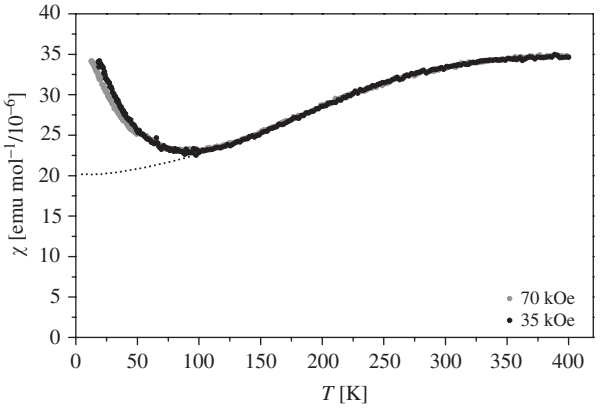

Fig. 3. Temperature dependence of the magnetic susceptibility of Ti_2PTe_2 (powder sample), the dotted line shows the extrapolation to $T = 0$ K.

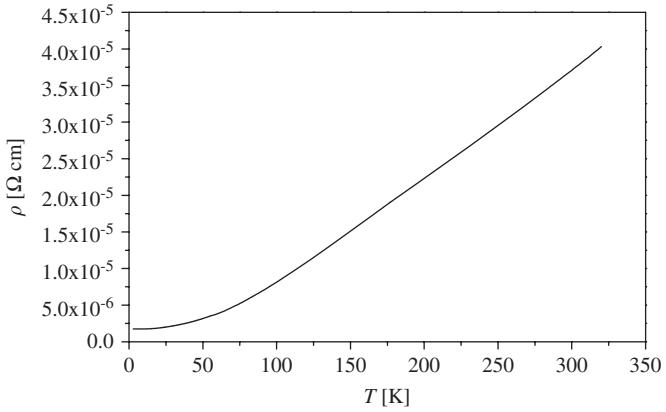

Fig. 4. Temperature dependence of the electrical resistivity of Ti_2PTe_2 within the hexagonal *ab*-plane.

metal (42 μΩ cm). The very low residual resistivity $\rho_0 \approx 0.8$ μΩ cm suggests a good crystal quality. The metallic conduction parallel to the hexagonal *ab*-planes is consistent with the observation of the Pauli term in susceptibility and the results of band structure calculations.

The occurrence of Pauli-paramagnetism and metallic conductivity in the compound Ti_2PTe_2 has to be explained by the existence of free electrons. If the proven existence of Ti^{4+} cations is considered, and P^{3-} and Te^{2-} anions are assumed, then neutrality is reached through one delocalised electron per formula unit. Furthermore, the overlap of Te–*p*-block bands and Ti–*d*-block bands could lead to metallic properties as found in $TiTe_2$ [64] (Fig. 4).

3.4. Quantum chemical calculations

The projected and total DOS plots for Ti_2PTe_2 are shown in Fig. 5. All atomic states are strongly mixed in the whole energy range. The Ti *d*-states and Te *p*-states mainly contribute to the DOS at the Fermi level, thus being responsible for the metallic behaviour of the compound.

The calculated band structure of Ti_2PTe_2 near the Fermi level is presented in Fig. 6 for the primitive rhombohedral cell, which constitutes one-third of a conventional hexagonal unit cell, therefore $Z_{\text{rhombohedral}} = 1$. The $(10\bar{1})$ and (111) directions in a rhombohedral cell chosen for the representation of the band structure correspond to the (100) and (001) directions in a

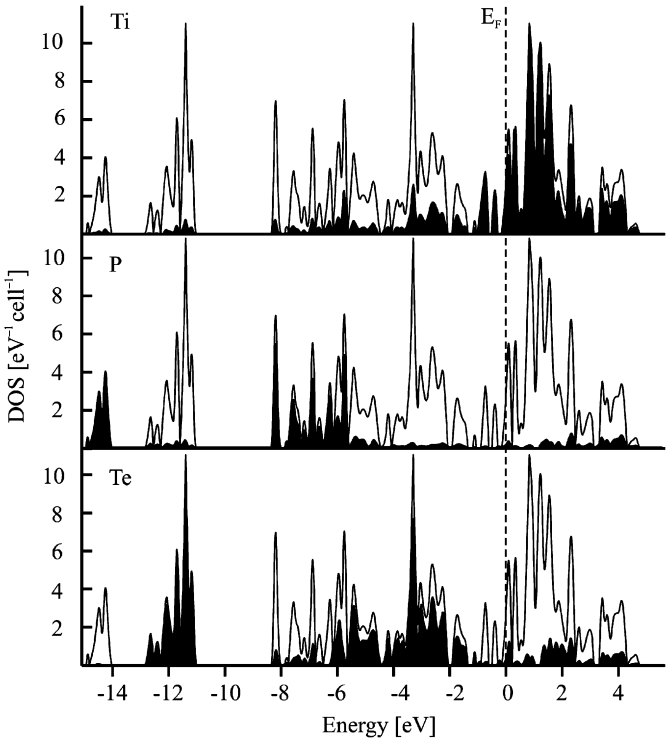

Fig. 5. The total (solid line) and projected (black filled) density of states for Ti_2PTe_2, calculated for the primitive rhombohedral cell with $Z_{\text{rhombohedral}} = 1$.

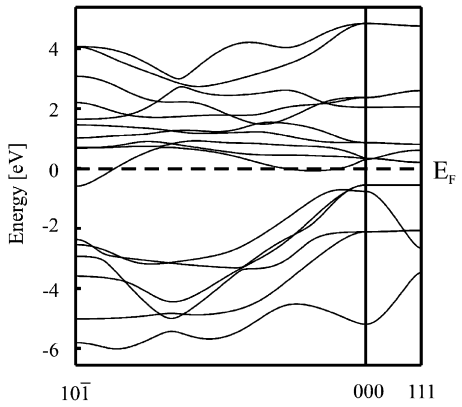

Fig. 6. The band structure of Ti_2PTe_2 along two directions in a primitive rhombohedral cell corresponding to the *a*- and *c*-axis of a conventional hexagonal cell.

hexagonal cell. The comparison of band dispersion along the *a*- and *c*-axis in the hexagonal setting reveals an evident anisotropy of bands that reflects the layered character of the crystal structure. One can expect metallic conductivity in the directions corresponding to the crystallographic *ab*-plane, i.e., the propagation of layers, although the DOS values at the Fermi level remain low. The evaluated DOS at the Fermi-level DOS(E_F) consists of ≈ 3 states eV^{-1} for the primitive rhombohedral cell, that is per one formula unit, and therewith does not differ very much from the experimental determined value of 5.3 states eV^{-1}. So the calculated band structure is in accordance with the results of the electrical conductivity measurements and the experimentally found Pauli-paramagnetic behaviour, the sharp peak of the DOS at the Fermi level explains the slight temperature dependence of the susceptibility. In the orthogonal direction to the *ab*-plane, the Fermi level resides in the narrow band gap that is

surely an effect of the van der Waals gap. Theoretically, the compound is predicted to be a two-dimensional metallic conductor, but the statement is not proved experimentally, since the true resistivity in *c* direction could not be measured due to internal short circuits.

4. Conclusion

The layered crystal structure of the new phosphide telluride Ti_2PTe_2 has been presented. The oxidation state +IV for titanium, corresponding to the formula $(Ti^{4+})_2(P^{3-})(Te^{2-})_2(e^-)$, is confirmed by XANES data. Metallic conductivity as well as Pauli-paramagnetism confirms the presence of free electrons. The anisotropy of the band structure reflects the layered type of crystal structure; the physical properties predicted from the calculations are consistent with the experimentally measured ones.

Supporting information

Further details of the crystal structure investigation can be obtained from the Fachinformationszentrum Karlsruhe, 76344 Eggenstein-Leopoldshafen, Germany (fax: +49 7247 808 666; e-mail: crysdata@fiz-karlsruhe.de) on quoting the depository number CSD 418978.

Acknowledgments

The authors thank Dr. Dariusz Zajac from HASYLAB, Hamburg, for his help during the XANES measurements. Financial support by the Deutsche Forschungsgemeinschaft and by the HASYLAB/DESY is gratefully acknowledged. A.I. greatly acknowledges the grant of an INTAS Young Scientists' Fellowship (ref. no. 05-109-4795) within the EU framework program.

References

[1] H. Kleinke, B. Harbrecht, Z. Anorg. Allg. Chem. 625 (1999) 1873.
[2] H. Kleinke, Chem. Commun. 2000 (2000) 1941.
[3] H. Kleinke, J. Alloy. Compds. 336 (2002) 132.
[4] A.J. Foecker, W. Jeitschko, J. Solid State Chem. 162 (2001) 69.
[5] T.K. Reynolds, J.G. Bales, F.J. DiSalvo, Chem. Mater. 14 (2002) 4746.
[6] A.J. Klein Haneveld, F. Jellinek, J. Less-Common Met. 18 (1969) 123.
[7] P. Jensen, A. Kjekshus, J. Less-Common Met. 13 (1967) 357.
[8] K. Deneke, A. Rabenau, Z. Anorg. Allg. Chem. 333 (1964) 201.
[9] R.L. Stegmann, E.A. Peretti, J. Inorg. Nucl. Chem. 28 (1966) 1589.
[10] S.S. Abdul Noor, J. Appl. Phys. 61 (1987) 3549.
[11] F.K. Lotgering, E.W. Gorter, J. Phys. Chem. Solids 3 (1957) 238.
[12] J. Rossat-Mignod, P. Burlet, S. Quezel, J.M. Effantin, D. Delacote, H. Bartholin, O. Vogt, D. Ravot, J. Magn. Magn. Mater. 31 (1983) 398.
[13] Y.C. Wang, K.M. Poduska, R. Hoffmann, F.J. DiSalvo, J. Alloy. Compds. 314 (2001) 132.
[14] T.K. Reynolds, R.F. Kelley, F.J. DiSalvo, J. Alloy. Compds. 366 (2004) 136.
[15] M.N. Abdusalyamova, A.G. Chuiko, A.Yu. Golubkov, S.I. Popov, L.S. Parfenova, A. Prokofiev, I.A. Smirnov, J. Alloy. Compds. 205 (1994) 107.
[16] W.-S. Kim, G.Y. Chao, Can. Mineral. 29 (1991) 401.
[17] P. Terzieff, H. Ipser, Monatsh. Chem. 123 (1992) 35.
[18] F. Hulliger, Mater. Res. Bull. 14 (1979) 259.
[19] R. Ferro, Z. Anorg. Allg. Chem. 275 (1954) 320.
[20] H.J. Whitfield, J. Solid State Chem. 39 (1981) 209.
[21] F. Hulliger, Z. Naturforsch. Part B 36 (1981) 463.
[22] F. Hulliger, T. Siegrist, Mater. Res. Bull. 16 (1981) 1245.
[23] A. Kjekshus, T. Rakke, Acta Chem. Scand. A 33 (1979) 609.
[24] J. Leciejewicz, A. Zygmunt, Phys. Status Solidi A 13 (1972) 657–660.
[25] R.M. Imamov, I.I. Petrov, Kristallografiya 13 (1968) 412.
[26] A. Kjekshus, W.E. Jamison, Acta Chem. Scand. A 25 (1971) 1715.
[27] H. Hahn, D. Thiele, Z. Anorg. Allg. Chem. 303 (1960) 147.
[28] R.B. Beeken, J.W. Schweitzer, Phys. Rev. B 23 (1981) 3620.
[29] F. Hulliger, G.W. Hull Jr., Solid State Commun. 8 (1970) 1379.
[30] A. Wojakowski, J. Less-Common Met. 107 (1985) 155.
[31] D. Pietraszko, K. Lukaszewicz, Bull. Acad. Pol. Sci. Ser. Sci. 23 (1975) 337.
[32] A. Mosset, Y.P. Jeannin, J. Less-Common Met. 26 (1972) 285.
[33] W. Bensch, W. Heid, J. Alloy. Compds. 224 (1995) 220.
[34] C.-C. Wang, C. Eylem, T. Hughbanks, Inorg. Chem. 37 (1998) 390.
[35] A. Mosset, Y.P. Jeannin, J. Solid State Chem. 7 (1973) 124.
[36] F.Q. Huang, P. Brazis, C.R. Kannewurf, J.A. Ibers, Inorg. Chem. 39 (2000) 3176.
[37] F.Q. Huang, C. Flaschenriem, P. Brazis, C.R. Kannewurf, J.A. Ibers, Inorg. Chem. 42 (2003) 3194.
[38] F. Hulliger, R. Schmelczer, D. Schwarzenbach, J. Solid State Chem. 21 (1977) 371.
[39] F. Hulliger, J. Less-Common Met. 16 (1968) 113.
[40] R. Wawryk, A. Wojakowski, A. Pietraszko, Z. Henkie, Solid State Commun. 133 (2005) 295.
[41] W. Jeitschko, Acta Crystallogr. B 30 (1974) 2565.
[42] P.C. Donohue, P.E. Bierstedt, Inorg. Chem. 8 (1969) 2690.
[43] A. Zygmunt, A. Murasik, S. Ligenza, J. Leciejewicz, Phys. Status Solidi A 22 (1974) 75.
[44] W.B. Pearson, Z. Kristallogr. 171 (1985) 23.
[45] G. Kliche, Z. Naturforsch. B 41 (1986) 130.
[46] H.D. Lutz, Th. Schmidt, G. Wäschenbach, Z. Anorg. Allg. Chem. 562 (1988) 7.
[47] S. Jörgens, D. Johrendt, A. Mewis, Chem. Eur. J. 9 (2003) 2405.
[48] F. Philipp, P. Schmidt, E. Milke, M. Binnewies, S. Hoffmann, J. Solid State Chem. 181 (2008) 758.
[49] G. Brauer, third ed, Handbuch der Präparativen Anorganischen Chemie, vol. 1, F. Enke Verlag Stuttgart, 1975, p. 506.
[50] H. Mayer, G. Pupp, Z. Kristallogr. 145 (1977) 321.
[51] X-Shape 1.06, Program for Crystal Optimization for Numerical Absorption Correction, STOE & Cie GmbH, Darmstadt, 1999.
[52] X-Red-32 1.01, Program for Data Reduction, STOE & Cie GmbH, Darmstadt, 2001.
[53] G.M. Sheldrick, SHELX-97, Program for Crystal Structure Determination, University of Göttingen, 1997.
[54] V.R. Saunders, R. Dovesi, C. Roetti, M. Causà, N.M. Harrison, R. Orlando, C.M. Zicovich-Wilson, CRYSTAL98 User's Manual, University of Torino, 1998.
[55] J. Hay, W.R. Wadt, J. Chem. Phys. 82 (1985) 284.
[56] S. Piskunov, E. Heifets, R.I. Eglitis, G. Borstel, Comput. Mater. Sci. 29 (2004) 165.
[57] S.V. Savilov, A.N. Kuznetsov, B.A. Popovkin, V.N. Khrustalev, P. Simon, J. Getzschmann, Th. Doert, M. Ruck, Z. Anorg. Allg. Chem. 631 (2005) 293;
A.A. Isaeva, A.I. Baranov, T. Doert, V.A. Kulbachinskii, P.V. Gurin, V.G. Kytin, V.I. Shtanov, J. Solid State Chem. 179 (2006) 4030.
[58] A. Kokalj, J. Mol. Graph. Model. 17 (1999) 176 Code available from 〈http://www.xcrysden.org/〉.
[59] D. Harker, Z. Kristallogr. 89 (1934) 175.
[60] J.A. Bland, S.J. Basinski, Can. J. Phys. 39 (1961) 1040.
[61] T.L. Anderson, H.B. Krause, Acta Crystallogr. B 30 (1974) 1307.
[62] A.H. Daane, R.E. Rundle, H.G. Smith, F.H. Spedding, Acta Crystallogr. 7 (1954) 532.
[63] H. Cordes, R. Schmid Fetzer, J. Alloy. Compds. 216 (1994) 197.
[64] E. Canadell, S. Jobic, R. Brec, J. Rouxel, M.-H. Whangbo, J. Solid State Chem. 99 (1992) 189.
[65] P.W. Selwood, Magnetochemistry, second ed, Interscience, New York, 1956.